Philosophical Magazine Letters,
Vol. 85, No. 2, February 2005, 67–75

Taylor & Francis
Taylor & Francis Group

Fractals and scaling in fracture induced by microcrack coalescence

C. LU*†‡, Y.-W. MAI† and Y. BAI‡

†Centre for Advanced Materials Technology (CAMT), School of Aerospace, Mechanical and Mechatronic Engineering J07, The University of Sydney, NSW 2006, Australia
‡State Key Laboratory of Nonlinear Mechanics (LNM), Institute of Mechanics, Chinese Academy of Sciences, Beijing 100080, P. R. China

(*Received 22 December 2004; in final form 26 April 2005*)

A numerical model is proposed to simulate fracture induced by the coalescence of numerous microcracks, in which the condition for coalescence between two randomly nucleated microcracks is determined in terms of a load-sharing principle. The results of the simulation show that, as the number density of nucleated microcracks increases, stochastic coalescence first occurs followed by a small fluctuation, and finally a newly nucleated microcrack triggers a cascade coalescence of microcracks resulting in catastrophic failure. The fracture profiles exhibit self-affine fractal characteristics with a universal roughness exponent, but the critical damage threshold is sensitive to details of the model. The spatiotemporal distribution of nucleated microcracks in the vicinity of critical failure follows a power-law behaviour, which implies that the microcrack system may evolve to a critical state.

1. Introduction

Most failures in disordered materials such as rock, ceramics, composites, etc., involve a variety of processes occurring over many scale lengths from microscopic to macroscopic. Generally speaking, catastrophic fracture in these materials is the result of a sequential process of nucleation, growth, and coalescence of numerous microcracks initiated at micro- (or nano-) scales. Material failure, as an important, typically nonlinear, dynamic phenomenon, has attracted much attention from physicists for a long time [1, 2]. Especially during the last two decades or so, several remarkably ''universal'' scaling behaviours in fracture processes have been discovered. For example, the fracture surface of metals was observed to exhibit fractal characteristics, and its topology is usually self-affine with universal roughness exponents [3–7]. Acoustic emission analyses of micro-fracture processes have revealed power-law distributions and critical phenomena [8–13]. All these discoveries can be viewed as hallmarks of the fracture process being a complex phenomenon with features of adaptation, self-organization and emergence.

*Corresponding author. Email: chunsheng.lu@aeromech.usyd.edu.au

Philosophical Magazine Letters
ISSN 0950–0839 print/ISSN 1362–3036 online
http://www.tandf.co.uk/journals
DOI: 10.1080/09500830500153917

To elucidate the underlying physical mechanisms in such a complex process, we must understand not only the threshold conditions that trigger this process, as in traditional fracture mechanics, but also the dynamics by which it proceeds. The concepts used for treating complex systems, such as those of fractals or multi-fractals, percolation, and renormalization group theory are instructive for the investigation of multi-scale fracture [14–17].

Several simple models, such as random-fuse and fibre-bundle-network models, have been proposed for pattern formation in deformation and fracture processes, in which the stress redistribution induced by failure of individual elements has been considered [18, 19]. Unfortunately, very large amounts of computer time, even on supercomputers, are required to obtain a cracking pattern containing just a few thousand broken bonds, owing to the lack of efficient algorithms. It seems unlikely that a substantial improvement can be made using presently available computer resources [18]. In addition, many aspects associated with the fracture process itself, especially in cases where disorder is important and may even govern the final catastrophic event, are still unclear [2, 20]. In this paper, a simple two-dimensional (2D) numerical model is proposed to simulate the fracture arising from the coalescence of randomly nucleated microcracks. We will concentrate mainly on the statistical properties of the collective evolution of numerous microcracks, and their spatiotemporal activity in the vicinity of a critical failure.

2. Model

Based on experimental findings, we developed a 2D evolution-induced catastrophe model to investigate the effect of disorder at the microscopic scale on a fracture process [21–23]. The model involves two main processes: microcrack nucleation and coalescence. The nucleated microcracks were randomly distributed on a 2D lattice, which contained various microstructures, such as second-phase particles, inclusions, and flaws etc. The coalescence condition between two neighbouring microcracks can be approximately determined by mechanical analysis. As an example, let us consider a simple dynamics of damage evolution, namely a load-sharing principle where the load supported by a broken part is shared by its two neighbouring intact parts. Here, the mean stress on the ligament with distance d between two neighbouring microcracks can be represented as $\bar{\sigma} = (1 + \bar{c}/d)\sigma_0$, where σ_0 is the nominal uniaxial stress and $\bar{c}$ is the average length of two microcracks (see figure 1). Provided that the angle θ between the orientation of two microcracks and the line joining their tips satisfies the condition $|\theta| \leq \pi/2$, the two neighbouring microcracks will coalesce when the mean stress $\bar{\sigma}$ achieves a critical value σ_c. Thus, the critical coalescence condition is given by:

$$r = \frac{d}{\bar{c}} \leq r_c = \frac{\sigma_0}{\sigma_c - \sigma_0}. \tag{1}$$

For simplicity, the probability of microcrack coalescence was assumed to be independent of the angle, θ, and the length of the coalesced crack was approximated by its projection normal to the loading direction. Furthermore, the stress level can be indirectly calculated from the crack density evolution *versus* time relationship.

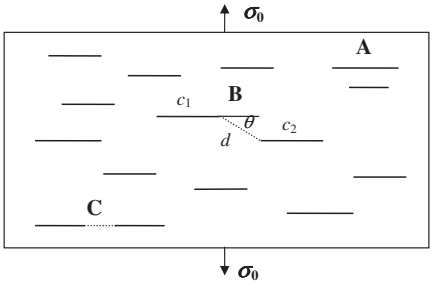

Figure 1. Schematic showing stacked microcracks nucleated, horizontally and randomly, in a two-dimensional lattice. Two microcracks shield and attract each other in cases A and C, respectively.

Here, it is noted that in order to understand easily the collective behaviour relating to the coalescence of microcracks, some simplifications or even oversimplifications were introduced in the model. More exactly, the coalescence condition in equation (1) should be calculated based on the stress intensity factors at each crack tip [24, 25]. Meanwhile, the nominal (normal or uniaxial) stress was assumed to be a scalar rather than a tensor through the geometrical approximation made for the coalesced microcracks. Clearly for some special structures of microcracks, such as a staircase-like distribution where the coalescence is mainly caused by the shear stress, suitable changes to the model are needed.

If the fundamental details of the damage evolution, for example, the size distribution of the nucleated microcracks and the coalescence conditions, are known, the model can be well applied to simulate a fracture process. In a case study on the spallation of an aluminium alloy at high-speed impact, the simulation results were in good agreement with the real crack patterns [21]. More details of the numerical model are discussed in references [22, 23]. The dynamics used in the simulations can be briefly summarized as follows:

(1) A newly nucleated microcrack is added randomly on a 2D lattice, with an orientation and length chosen from a given size distribution.
(2) The coalescence condition of equation (1) for a newly nucleated crack with all pre-existing ones, is checked in turn, starting from the closest pair. If the left tip of the new crack is located below or above the right tip of an existing crack (or *vice versa*), it is assumed that the new crack is shielded by the old one, and coalescence will not occur.
(3) Step (2) is repeated until there are no more cracks satisfying the coalescence condition and, at the same time, there is no crack spanning the whole lattice. Then, one returns to step (1).

3. Results

A typical damage evolution process in a 1000×1000 lattice is shown in figure 2, where a uniform length distribution of nucleated microcracks with a mean length of 2 (lattice units) and a critical coalescence condition $r_c = 1$ were used in the simulation

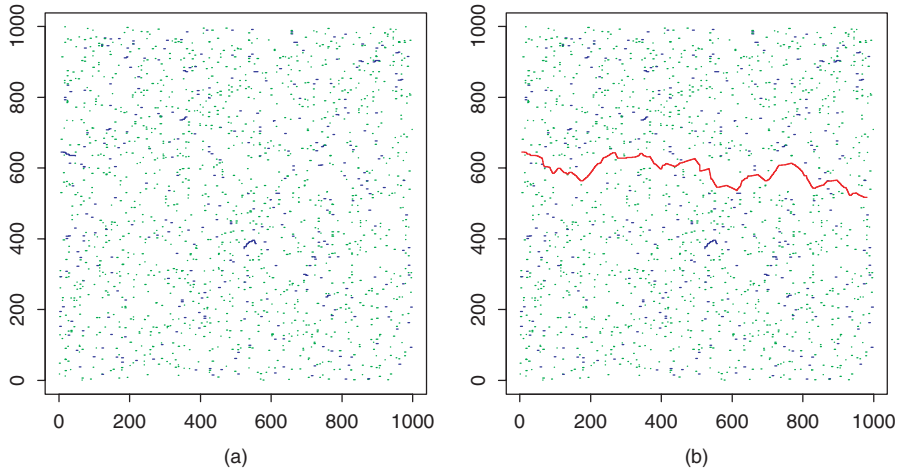

Figure 2. Patterns of microcrack coalescence in a 1000×1000 lattice: (a) just before fracture; and (b) a newly nucleated microcrack triggers the catastrophic failure.

study [23]. It is obvious that there are three different phases (stages) in this process. (i) An initial phase in which nucleated microcracks are too sparse to cause coalescence, and the number of microcracks increases linearly with time; (ii) a stable phase in which a significant proportion of newly nucleated microcracks fall close enough to an existing crack-tip to cause coalescence. Such a coalescence event has two effects: (a) it enlarges the influence zone around the crack-tip and so increases the chance of a coalescence event, and (b) it increases the area shielded by the coalesced crack. In the latter case, if a new microcrack appears in the shielded region, it does not coalesce. These two effects balance each other producing a near-stable regime. (iii) A critical phase: after a certain time, the influence zones extend and overlap to such an extent that a newly nucleated microcrack (a small fluctuation) will trigger a cascade coalescence of microcracks and result in a catastrophic failure (an avalanche). However, we cannot predict, *a priori*, the exact position at which the final fracture will appear (figure 2).

As is well known, fractography is a useful tool to examine possible failure mechanisms of a material since the fracture surface more or less records the features created during the fracture process. For a given fracture surface, the roughness index (Hurst exponent) ζ is defined by:

$$w = \langle \max h_i(x') - \min h_i(x') \rangle \sim L^{\varsigma}, \tag{2}$$

where $h_i(x')$ is the height of the fracture profile in a window with length L, and $x' \in (x,\ x+L)$. The roughness exponent ζ lies between the values 0 and 1, and is related to the fractal dimension d_f via the relation, $d_f = D - \zeta$, where D is the Euclidean dimension [7]. In their pioneering work, Mandelbrot *et al.* [3] showed that the fracture surface of metals exhibits fractal characteristics, and that the fractal dimension can be used as a measure of both the roughness of the fracture surface and the fracture toughness. It was conjectured that the value of roughness exponent $\zeta \approx 0.8$ (usually between 0.7 and 0.9 in most experiments) is likely to be a universal

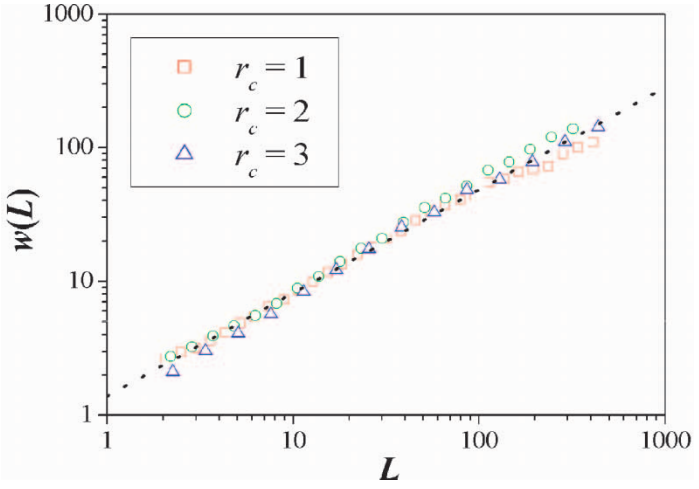

Figure 3. Log–log plot of fracture profile roughness $w(L)$ *versus* window size L for three cases of different critical coalescence conditions: $r_c = 1$, 2, and 3, where the fitted slope using equation (2) (dotted line) is $\zeta = 0.77 \pm 0.02$.

exponent in the micro-scale range, whereas $\zeta \approx 0.5$ in the nanoscale range. This is, however, still a controversial topic [7].

As shown in figure 3, there is indeed such a power-law, $w \sim L^{\zeta}$ with $\zeta = 0.77 \pm 0.02$, which seems independent of the details used in the model, such as the size distribution function of the nucleated microcracks (this is whether it is uniform, normal, Weibull, power-law, or exponential with a given characteristic length) and the critical coalescence conditions [21, 22]. Thus, the fracture surface obtained from simulations has self-affine fractal characteristics. Several models were suggested to describe the universal range, but there is still no clear physical picture why the roughness exponent should be about 0.8 in the micro-scale range [6, 26, 27]. In particular, the universal range of these power laws in different dimensions should be further studied, such as in reference [28].

It is worth noting that the results cannot be directly extended to cases with the extremely critical coalescence conditions $r_c \ll 1$ or $r_c \gg 1$ [22]. Intuitively, such a microcrack evolution process is very similar to percolation, and final catastrophic failure corresponds to the occurrence of an infinite cluster at the critical concentration [14]. This leads to another interesting parameter, namely the damage at critical failure, which can be defined as either the accumulative number or the length (area or volume in three-dimensional case) of the nucleated microcracks. Here, we use the former of these definitions. As shown in figure 4, the threshold damage value is not a constant as in conventional percolation, but is sensitive to details of the model. The threshold density of the number of accumulated crack at $r_c = 1$ follows a normal distribution with a mean $\bar{n}_c = 1731.29$ and standard deviation $\sigma_\rho = 424.47$ (see inset in figure 4). The smaller the value of r_c, the narrower is the variance of threshold damage distribution. Thus, percolation can be viewed as an approximation to the fracture process in an extremely disordered media, i.e., $r_c \ll 1$. In fact, as indicated

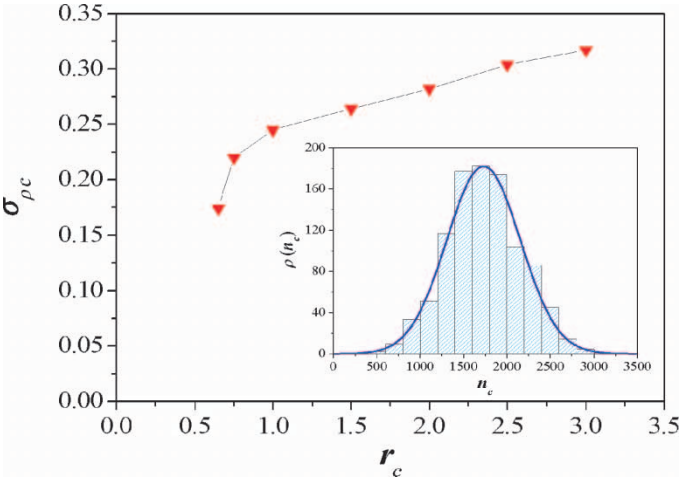

Figure 4. The relative deviation $\sigma_{\rho c}$ (the standard deviation/mean ratio) of threshold density distribution *versus* the coalescence condition r_c, where the inset shows the density distribution of the threshold number of nucleated microcracks in 1000 simulations ($r_c = 1$) with the mean $\bar{n}_c = 1731.29$ and the standard deviation $\sigma_\rho = 424.47$.

by equation (1), fracture induced by microcrack coalescence is controlled by the non-local, long-range, stress redistribution.

Next, we focus attention on the final stage of damage evolution and examine whether fracture is a kind of critical phenomena. Or conversely, we ask to what extent the predictability of a final catastrophic failure is dependent on the sensitivity of the microcrack system to disorder or stochastic fluctuation [29, 30]. For this purpose, we just randomly change the spatial position of the nucleated microcrack that induces the avalanche (catastrophic failure), and observe the spatiotemporal distribution. That is, we wish to find both the waiting time to the next critical point and the new spatial position of a microcrack that triggers the final avalanche. For simplicity, we assume that the waiting time is proportional to the number of nucleated microcracks. As shown in figure 5, the waiting time decays exponentially, but there is a long tail of power-law type over a large time interval Δt. The cumulative distribution of waiting time can be described by:

$$N(>\Delta t) \sim (\Delta t)^{-\gamma}[1 + \exp(-\varepsilon \Delta t)], \tag{3}$$

where $\varepsilon \approx 0.0045$. Thus the exponential term is important only for the small time interval Δt, and the time region of importance is about equal to the variation of the critical crack numbers (see inset in figure 4). Far from this domain, we have a power-law distribution, $N(>\Delta t) \sim (\Delta t)^{-\gamma}$. Moreover, the spatial positions of the next critical microcracks are not uniform, and the cluster distribution follows a power-law, $N(r) \sim r^{-\alpha}$ with $\alpha \approx 1$, where r is the coarse-grained size and $N(r)$ is the number of windows in which there is at least one critical micro-crack (see figure 6). Here, the spatiotemporal power-law scaling strongly implies that the collective evolution through microcrack coalescence may be at a critical state [31, 32].

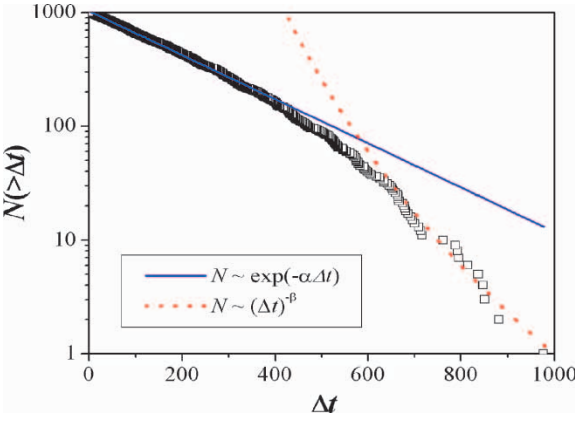

Figure 5. Cumulative number distribution of newly nucleated microcracks Δn (that is, difference from the original critical number) in 1000 simulations with critical coalescence condition $r_c = 1$. As Δt (here, $\Delta t \sim \Delta n$) increases, the distribution decays by an exponential law (solid line, $\varepsilon \approx 0.0045$), but follows a power-law (dotted line, $\gamma \approx 8.0$) for large Δt.

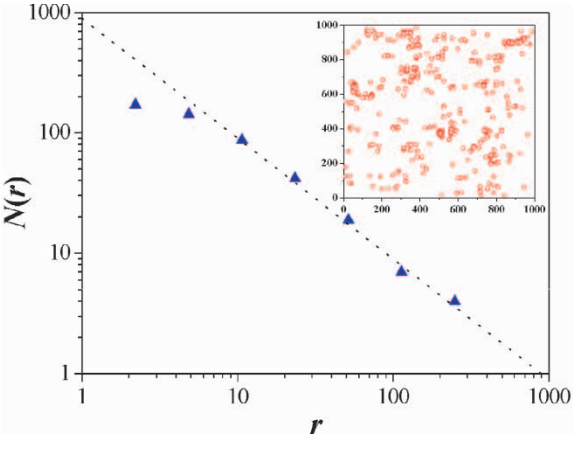

Figure 6. Spatial distribution of critical nucleated microcracks *versus* coarse-grained length r in 1000 simulations with critical coalescence condition $r_c = 1$, where the slope of dotted line is -1. The inset shows the spatial pattern of nucleated microcracks that trigger catastrophic failure.

Unlike sand-piles models, the driving force here is a newly nucleated microcrack per time-step from a prescribed distribution, which is randomly distributed in the lattice.

4. Discussion and conclusions

We briefly discuss the implications of these results for the predictability of a catastrophic failure. As we know, a self-organized critical system lies on the verge

of chaos, where the uncertainty grows algebraically rather than exponentially. That is, our ability to forecast is gradually lost, but much more slowly than for a chaotic system [33]. In some sense, catastrophic failure due to the coalescence of numerous microcracks can be imagined to be a snapshot of self-organized critical phenomena. Thus, it may still be possible to predict some properties in the catastrophic fracture of disordered media. For instance, some precursors approaching critical failure were found from an analysis of acoustic emission signals [8, 10]. Also discovered were several general features that might be significantly enhanced near catastrophic failure [29, 30]. Furthermore, the scaling behaviours, as discussed above, highlight the possibility that the material property at the macroscopic scale could be insensitive to details on the microscale. Recent studies indeed showed that the strengths of electroceramics, like zinc oxide, became insensitive to flaws at the micro-scale because of the influence and interaction of various factors [34, 35]. However, the flaw tolerance concept cannot be considered to be of general validity, even at the nanoscale, as demonstrated in [36].

In conclusion, a simple numerical model has been proposed to simulate the fracture process due to the collective evolution of numerous microcracks. Simulation results show that fracture profiles exhibit self-affine fractal characteristics, and their roughness exponents are likely to have a universal value, which is independent of details used in the model, such as the size distribution of nucleated microcracks, coalescence conditions, etc. However, in contrast to traditional percolation theory, the critical damage threshold is sensitive to the details, and the spatial position of a microcrack triggering the final fracture cannot be predicted *a priori*. The spatiotemporal distribution of nucleated microcracks in the vicinity of critical failure follows a power-law scaling, and the system may lie in a critical state, which sheds some light on the predictability of catastrophic fracture in disordered materials.

Acknowledgements

We are grateful to H. Takayasu and D. Vere-Jones for instructive discussions. This work was supported by the Australian Research Council (ARC) and the National Natural Science Foundation of China. YWM and CL are, respectively, Australian Federation Fellow and ARC Senior Research Associate.

References

[1] D.R. Curran, L. Seaman and D.A. Shockey, Phys. Rep. **147** 253 (1987).
[2] F. Fineberg and M. Marder, Phys. Rep. **313** 1 (1999).
[3] B.B. Mandelbrot, D.E. Passoja and A.J. Paullay, Nature **308** 721 (1984).
[4] R. Cahn, Nature **338** 201 (1989).
[5] H. Takayasu, *Fractals in the Physical Sciences* (Manchester University Press, Manchester, 1990).
[6] E. Bouchaud, G. Lapasset and J. Planès, Europhys. Lett. **13** 73 (1990).
[7] E. Bouchaud, J. Phys.: Condens. Matter **9** 4319 (1997).
[8] G. Caldarelli, F.D. Di Tolla and A. Petri, Phys. Rev. Lett. **77** 2503 (1996).
[9] L. Mishnaevsky Jr, Engng Fract. Mech. **56** 47 (1997).

[10] A. Garcimartin, A. Guarino, L. Bellon and S. Ciliberto, Phys. Rev. Lett. **79** 3202 (1997).
[11] S. Zapperi, P. Ray, H.E. Stanley and A. Vespignani, Phys. Rev. Lett. **78** 1408 (1997).
[12] S. Zapperi, A. Vespignani and H.E. Stanley, Nature **388** 658 (1997).
[13] J.P. Sethna, K.A. Dahmen and C.R. Myers, Nature **410** 242 (2001).
[14] H.J. Herrmann and S. Roux (Editors), *Statistical Models for the Fracture of Disordered Media* (North-Holland, Amsterdam, 1990).
[15] A. Carpinteri, Int. J. Solids Struct. **31** 291 (1994).
[16] X. Diao and Y.-W. Mai, Phil. Mag. Lett. **79** 187 (1999).
[17] A. Carpinteri, P. Cornetti, F. Barpi and S. Valente, Engng Fract. Mech. **70** 1809 (2003).
[18] P. Meakin, Science **252** 226 (1991).
[19] C. Lu, H. Takayasu, A.Y. Tretyakov, M. Takayasu and S. Yumoto, Phys. Lett. A **242** 349 (1998).
[20] G.I. Barenblatt, in *Theoretical and Applied Mechanics*, edited by S.R. Bodner, J. Singer, A. Solan and Z. Hashin (North-Holland, Amsterdam, 1993).
[21] Y. Bai, C. Lu, F. Ke and M. Xia, Phys. Lett. A **185** 196 (1994).
[22] C. Lu, F. Ke, Y. Bai and M. Xia, Sci. China A **38** 462 (1995).
[23] C. Lu, D. Vere-Jones and H. Takayasu, Phys. Rev. Lett. **82** 347 (1999).
[24] A. Carpinteri and G.P. Yang, Theor. Appl. Fract. Mech. **25** 73 (1996).
[25] A. Carpinteri, F. Ciola and N. Pugno, Comput. Struct. **79** 389 (2001).
[26] G.G. Batrouni and A. Hansen, Phys. Rev. Lett. **80** 325 (1998).
[27] V.I. Räisänen, E.T. Seppala, M.J. Alava and P.M. Duxbury, Phys. Rev. Lett. **80** 329 (1998).
[28] A. Carpinteri and N. Pugno, J. appl. Mech. **69** 854 (2002).
[29] M. Xia, F. Ke, J. Bai and Y. Bai, Phys. Lett. A **236** 60 (1997).
[30] M. Xia, Y. Wei, F. Ke and Y. Bai, Pure appl. Geophys. **159** 2491 (2002).
[31] P. Bak, C. Tang and K. Wiesenfeld, Phys. Rev. Lett. **59** 381 (1987).
[32] D.L. Turcotte, Rep. Prog. Phys. **62** 1377 (1999).
[33] P. Bak, *How Nature Works: The Science of Self-Organized Criticality* (Springer, New York, 1996).
[34] C. Lu, R. Danzer and F.D. Fischer, Phys. Rev. E **65** 067102 (2002).
[35] C. Lu, R. Danzer and F.D. Fischer, J. Eur. Ceram. Soc. **24** 3643 (2004).
[36] N. Pugno and R. Ruoff, Phil. Mag. **84** 2829 (2004).